Soft Bending Modes of Terminal Chlorides in Gaseous Two- and Three-Coordinate Cu(II)−Cl Species

Beate K. Ystenes[†]

Department of Inorganic Chemistry, Norwegian University of Science and Technology (NTNU), N-7491 Trondheim, Norway

Vidar R. Jensen*

Max-Planck-Institut für Kohlenforschung, Kaiser-Wilhelm-Platz 1, D-45470 Mülheim an der Ruhr, Germany

Received March 5, 1999

The structures and vibrational spectra of the monomer and dimer of copper dichloride as well as the 1:1 complexes with aluminum and gallium trichloride, $CuAlCl_5$ and $CuGaCl_5$, have been studied using ab initio and density functional methods. For all molecules, equilibrium structures corresponding to minima on the potential energy surface were found to possess the ideal and expected $D_{\infty h}$, D_{2h}, or C_{2v} symmetries, respectively. These complexes are, however, easily distorted through bending of the terminal chlorines connected to copper in the plane of the singly occupied orbital in Cu d^9. Calculated bending potentials show that the corresponding modes are very soft. For the higher associates of $CuCl_2$, vibrational bands that may facilitate the verification of the structures are presented.

Introduction

Metal halides are well-known to form polymeric or complex species in the vapor phase above the condensed phase. In this work, we study monomeric and dimeric copper chloride as well as the 1:1 complexes between $CuCl_2$ and $AlCl_3$ or $GaCl_3$.

The earliest report on gaseous Cu_2Cl_4 was in an IR study by Leroi et al.[1] Later Papatheodorou[2] and Dienstbach et al.[3] published results from resonance Raman investigations, which support a trigonal configuration for the copper atom. All of the reports assume the molecule to have a ring structure with D_{2h} symmetry. The same symmetry is assumed for a large number of dimers of metal dihalides, but such structures have only recently been verified, e.g., for Be_2Cl_4,[4] Mg_2Cl_4,[5] and Ca_2Cl_4.[6] For all of these, the perfect D_{2h} symmetry seems to be in accordance with both experimental[7−11] and theoretical results,[5,12,13] but no experimental or theoretical work so far gives conclusive evidence concerning the structure of Cu_2Cl_4.

Chemical vapor transport for purification of metal halides is often accomplished with the help of complexing halides, in particular $AlCl_3$ and its congeners. This leads to a multitude of gas-phase complexes, among them $CuAlCl_5$ and $CuGaCl_5$ which are included in this work. Papatheodorou and Capote[14] proved the existence of $CuAlCl_5$ by means of resonance Raman spectroscopy and suggested a C_{2v} ring structure with three-coordinate copper and four-coordinate aluminum. Schläpfer and Rohrbasser[15] have observed $CuGaCl_5$ in their resonance Raman spectra, but assigned all of its bands to $CuGa_2Cl_8$. The verification of the structures of these complexes, along with an interpretation of their vibrational spectra, is therefore a prime goal of the present work.

It has proven difficult to determine the ground electronic state and geometry of $CuCl_2$ as well as a number of other transition metal dihalides (cf. Hargittai[16]), and in recent years a number of gas-phase investigations of $CuCl_2$ have been reported,[17−24]

* To whom correspondence should be addressed.
[†] New address: School of Technology, Sør-Trøndelag College, N-7005 Trondheim, Norway.

(1) Leroi, G. E.; James, T. C.; Hougen, J. T.; Klemperer, W. *J. Chem. Phys.* **1962**, *36*, 2879.
(2) Papatheodorou, G. N. *NBS Spec. Publ. (U.S.)* **1979**, *561-1*, 647.
(3) Dienstbach, F.; Emmenegger, F. P.; Schläpfer, C. W. *Helv. Chim. Acta* **1977**, *60*, 2460.
(4) Girichev, A. G.; Giricheva, N. I.; Vogt, N.; Girichev, G. V.; Vogt, J. *J. Mol. Struct.* **1996**, *384*, 175.
(5) Molnár, J.; Marsden, C. J.; Hargittai, M. *J. Phys. Chem.* **1995**, *99*, 9062.
(6) Vajda, E.; Hargittai, M.; Hargittai, I.; Tremmel, J.; Brunvoll, J. *Inorg. Chem.* **1987**, *26*, 1171.
(7) Büchler, A.; Klemperer, W. *J. Chem. Phys.* **195**, *29*, 121.
(8) Snelson, A. *J. Phys. Chem.* **1966**, *70*, 3208; *J. Phys. Chem.* **1968**, *72*, 250.
(9) Lesiecki, M. L.; Nibler, J. W. *J. Chem. Phys.* **1976**, *64*, 871.
(10) Cocke, D. L.; Chang, C.-A. L.; Gingerich, K. A. *Appl. Spectrosc.* **1973**, *27*, 260.
(11) Ramondo, F.; Bencivenni, L.; Nunziante Cesaro, S.; Hilpert, K. *J. Mol. Struct.* **1989**, *192*, 83.
(12) Ystenes, B. K. *Spectrochim. Acta, Part A* **1998**, *54*, 855.
(13) Ystenes, B. K. *Spectrochim. Acta, Part A*, to be submitted.
(14) Papatheodorou, G. N.; Capote, M. A. *J. Chem. Phys.* **1978**, *69*, 2067. See also ref 2.
(15) Schläpfer, C. W.; Rohrbasser, C. *Inorg. Chem.* **1978**, *17*, 1623.
(16) Hargittai, M. *Coord. Chem. Rev.* **1988**, *91*, 35.
(17) Bouvier, A. J.; Bacis, R.; Bonnet, J.; Churassy, S.; Crozet, P.; Erba, B.; Koffend, J. B.; Lamarre, J.; Lamrini, M.; Pigache, D.; Ross, A. J. *Chem. Phys. Lett.* **1991**, *184*, 133.
(18) Ross, A. J.; Bacis, R.; Bouvier, A. J.; Churassy, S.; Coste, J.-C.; Crozet, P.; Russier, I. *J. Mol. Spectrosc.* **1993**, *158*, 27.
(19) Barnes, M. P.; Carter, R. T.; Lakin N. M.; Brown, J. M. *J. Chem. Soc., Faraday Trans.* **1993**, *89*, 3205.
(20) Crozet, P.; Coste, J. C.; Bacis, R.; Bouvier, A. J.; Churassy, S.; Ross, A. *J. Chem. Phys.* **1993**, *178*, 505.
(21) Crozet, P.; Ross, A. J.; Bacis, R.; Barnes, M. P.; Brown, J. M. *J. Mol. Spectrosc.* **1995**, *172*, 43.

10.1021/ic990270m CCC: $18.00
Published on Web 08/13/1999

focusing on the rovibrational structure in selected parts of the electronic spectrum. Agreement between theory and experiment seems to have been reached concerning the ground state and vital parts of the electronic spectrum for this molecule.[24,25] On the other hand, there exist experimental indications of both linear[24] and bent[2,3] $CuCl_2$, and the shape of the molecule has yet to be studied explicitly by quantum chemical methods. Quantum chemistry may assist in the interpretation of the electronic and vibrational spectra[25,26] of the transition metal dihalides, as well as afford information about the potential curves of bending, as recently seen for $CrCl_2$.[26] To address the shape of $CuCl_2$ by means of calculated potential curves of bending and analysis of the vibrational spectrum is thus another goal of the present contribution. As this problem turned out to be particularly complex, we found it necessary to give it a broad treatment, also to have a sound reference for our work on the larger molecules.

Computational Details

Geometry Optimizations and Vibrational Analyses. Geometry optimizations by means of analytically obtained gradients were performed using the Hartree−Fock (HF) method, and also with Becke's three-parameter hybrid density functional[27] (B3LYP) as implemented in the Gaussian 94 suite of programs.[28] The density was evaluated using a grid with 75 radial shells per atom and 302 angular points per shell in the B3LYP calculations. The HF geometry optimizations were performed within the restricted open shell (ROHF) or unrestricted (UHF) formalism as indicated in each case. The Gamess[29] set of programs was used for these calculations, and geometries were converged to a maximum gradient below $1 \times 10^{-4} E_h/a_0$. The optimizations using the B3LYP method were performed within the unrestricted formalism (restricted for $AlCl_3$) using the Gaussian 94 package.[28] Geometries were converged to maximum gradient and displacement of $4.5 \times 10^{-4} E_h/a_0$ and $1.8 \times 10^{-3} a_0$, respectively. All stationary points obtained through full optimization within a given symmetry were characterized by the curvature of the potential energy surface. Using the B3LYP method, the Hessian matrices were obtained analytically, while numerical differentiation was performed in the case of HF. All frequencies were obtained within the harmonic approximation. Potential energy curves of bending were obtained through optimizations (using B3LYP) with constrained bending angle.

For $CuCl_2$, geometry optimizations were also performed at the UCCSD(T) (coupled cluster with single and double substitutions[30−33] of the UHF reference, and with a perturbative estimate of connected triples[34]) level with numerically obtained gradients. The Gaussian 94 package[28] was used, and the convergence criteria were as for the B3LYP optimizations described above. All valence electrons were correlated in the UCCSD(T) calculations.

Cartesian basis functions, retaining the s contaminant of d shells, were used in all geometry optimizations at the HF and B3LYP levels in the present work. For copper, the Wachters[35] primitive basis contracted to [10s,8p,3d] with the standard modifications as implemented in Gamess[29] was used. 6-31G[36] bases were used for chlorine and aluminum, while gallium was described by a Binning−Curtiss[37] (14s,11p,5d)/[6s,4p,1d] contracted basis. All basis sets for the main-group atoms were augmented by polarization functions ($\alpha_d = 0.75$, 0.325, and 0.207 for chlorine, aluminum, and gallium, respectively).[38] For simplicity, these basis sets, including the metal sets, are termed 6-31G(d) in the present work. Earlier studies have shown that the above-described basis sets are well suited for investigation of geometry and vibrational frequencies for Al_2Cl_6[39,40] and Ga_2Cl_6.[41]

For $CuCl_2$, the geometry optimizations at the UCCSD(T) level were performed with basis sets termed TZD2P in the present work. These sets were constructed from spherical harmonic functions. For Cu, the Wachters primitive basis[35] was augmented by two primitive 4p exponents, a diffuse d exponent ($\alpha_d = 0.1491$), and a (3f) set.[42] The contraction of the innermost (14s,9p,4d) followed Wachters's scheme 3. The two outermost p and d exponents were left uncontracted, while the f primitives were contracted to [2f], leading in total to a [8s,6p,4d,2f] contracted set. Chlorine was described by a Huzinaga primitive (12s,9p) basis contracted according to McLean and Chandler's chloride scheme[43] to [6s,5p]. Diffuse s and p functions were added in an even-tempered fashion along with two uncontracted d functions ($\alpha_d = 1.299$, 0.433).

Energy Evaluations. Single point energy calculations, in B3LYP-optimized geometries, were performed with the B3LYP method (see above), at the HF (RHF and ROHF) level of theory as well as with a couple of approaches based on configuration interaction (CI). The CI methods chosen were the modified coupled pair functional (MCPF) approximation,[44] as well as spin-adapted[45,46] RCCSD(T) (coupled cluster with single and double substitutions[30−33] of the RHF reference, and with a perturbative estimate of connected triples[34]).

MCPF is a size-consistent single-reference state method with the zeroth-order wave function defined at the RHF (or ROHF) level. The MCPF calculations were performed using the Stockholm set of programs.[47] All valence electrons were correlated, except those of 3s on chlorine. The core orbitals, as well as 3s on chlorine, were localized according to a $\langle r^2 \rangle$ minimization procedure[48] prior to the correlation treatment. The RCCSD(T) calculations were performed with the MOLCAS-4 set of programs,[49] and all valence electrons were correlated in the RCCSD(T) calculations.

(22) Bouvier, A. J.; Bosch, E.; Bouvier, A. *Chem. Phys.* **1996**, *202*, 139.
(23) Ross, A. J.; Crozet, P.; Bacis, R.; Churassy, S.; Erba, B.; Ashworth, S. H.; Lakin, N. M.; Wickham, M. R.; Beattie, I. R.; Brown, J. M. *J. Mol. Spectrosc*. **1996**, *177*, 134.
(24) Beattie, I. R.; Brown, J. M.; Crozet, P.; Ross A. J.; Yiannopoulou, A. *Inorg. Chem.* **1997**, *36*, 3207.
(25) Bauschlicher, C. W., Jr.; Roos, B. O. *J. Chem. Phys.* **1989**, *91*, 4785.
(26) Jensen, V. R. *Mol. Phys.* **1997**, *91*, 131.
(27) Becke, A. D. *J. Chem. Phys.* **1993**, *98*, 5648.
(28) Frisch, M. J.; Trucks, G. W.; Schlegel, H. B.; Gill, P. M. W.; Johnson, B. G.; Robb, M. A.; Cheeseman, J. R.; Keith, T. A.; Petersson, G. A.; Montgomery, J. A.; Raghavachari, K.; Al-Laham, M. A.; Zakrzewski, V. G.; Ortiz, J. V.; Foresman, J. B.; Cioslowski, J.; Stefanov, B. B.; Nanayakkara, A.; Challacombe, M.; Peng, C. Y.; Ayala, P. Y.; Chen, W.; Wong, M. W.; Andres, J. L.; Replogle, E. S.; Gomperts, R. R.; Martin, L.; Fox, D. J.; Binkley, J. S.; Defrees, D. J.; Baker, J.; Stewart, J. P.; Head-Gordon, M.; Gonzalez, C.; Pople, J. A. *Gaussian 94*, revision B.3; Gaussian, Inc.: Pittsburgh, PA, 1995.
(29) Schmidt, M. W.; Baldridge, K. K.; Boatz, J. A.; Elbert, S. T.; Gordon, M. S.; Jensen, J. J.; Koseki, S.; Matsunaga, N.; Nguyen, K. A.; Su, S.; Windus T. L.; Dupuis, M.; Montgomery, J. A. *J. Comput. Chem.* **1993**, *14*, 1347.
(30) Cizek, J. *Adv. Chem. Phys.* **1969**, *14*, 35.
(31) Purvis, G. D.; Bartlett, R. J. *J. Chem. Phys.* **1982**, *76*, 1910.
(32) Scuseria, G. E.; Janssen, C. L.; Schaefer, H. F., III. *J. Chem. Phys.* **1988**, *89*, 7382.
(33) Scuseria, G. E.; Schaefer, H. F., III. *J. Chem. Phys.* **1989**, *90*, 3700.
(34) Pople, J. A.; Head-Gordon, M.; Raghavachari, K. *J. Chem. Phys.* **1987**, *87*, 5968.
(35) Wachters, A. J. H. *J. Chem. Phys.* **1970**, *52*, 1033.
(36) Francl, M. M.; Pietro, W. J.; Hehre, W. J.; Binkley, J. S.; Gordon, M. S.; DeFrees, D. J.; Pople, J. A. *J. Chem. Phys.* **1982**, *77*, 3654.
(37) Binning, R. C., Jr.; Curtiss, L. A. *J. Comput. Chem*. **1990**, *11*, 1206.
(38) Hariharan, P. C.; Pople, J. A. *Theor. Chim. Acta* **1973**, *28*, 213.
(39) Mains, G. J.; Bock, C. W.; Trachmann, M.; Mastryukov, V. S. *J. Mol. Struct.* **1992**, *274*, 277.
(40) Ystenes, M.; Rytter, E.; Menzel, F.; Brockner, W. *Spectrochim. Acta, Part A* **1994**, *50*, 233.
(41) Ystenes, M.; Westberg, N.; Ehrhardt, B. K. *Spectrochim. Acta, Part A* **1995**, *51*, 1017.
(42) Bauschlicher, C. W., Jr.; Langhoff, S. R.; Barnes, L. A. *J. Chem. Phys*. **1989**, *91*, 2399.
(43) McLean, A. D.; Chandler, G. S. *J. Chem. Phys.* **1980**, *72*, 5639.
(44) Chong, D. P.; Langhoff, S. R. *J. Chem. Phys.* **1986**, *84*, 5606.
(45) Neogrády, P.; Urban, M.; Hubac, I. *J. Chem. Phys.* **1992**, *97*, 5074.
(46) Neogrády, P.; Urban, M.; Hubac, I. *J. Chem. Phys.* **1994**, *100*, 3706.
(47) Siegbahn, P. E. M.; Blomberg, M. R. A.; Pettersson, L. G. M.; Roos B. O.; Almlöf, J. *STOCKHOLM*; University of Stockholm: Stockholm, Sweden, 1995.
(48) Pettersson, L. G. M.; Åkeby, H. *J. Chem. Phys.* **1991**, *94*, 2968.

Scaling of the correlation energy has been adopted as a scheme for obtaining better estimates of relative energies in the present study. The strategy used is the PCI-*X* scheme according to Siegbahn et al.,[50] where *X* is the percentage of the correlation effects that the parent CI method is expected to account for. The PCI-*X* scheme was originally developed for scaling of correlation energies obtained with the MCPF method in conjunction with bases of double-ζ plus polarization (DZP) quality, for which the optimal value of *X* was found to be close to 78.[51] An improved estimate of relative energies is thus obtained by adding 22% of the difference between the SCF energy and the total extrapolated energy. With the CCSD(T) method, *X* increases to 80,[51] still referring to bases of DZP quality. The latter scheme, PCI-80(CCSD(T)), in connection with basis sets (termed 6-31+G(d)) to be detailed below, is expected to be the most reliable approach with which energy differences are calculated in the current work. A comparison in the Appendix confirms excellent agreement between bending potentials calculated with PCI-80(CCSD(T))/6-31+G(d) and CCSD(T) using large atomic natural orbital (ANO) sets.

Estimates of scalar relativistic effects were included in all energy evaluations in the present work. The corrections were obtained using first-order perturbation theory including the mass−velocity and Darwin terms.[52,53] For technical reasons, no MCPF calculations could be performed for Cu_2Cl_4, and the construction of relative energies involving this molecule was thus based on relativistic corrections taken from HF calculations. For all of the other molecules, the corrections were obtained from the MCPF density. The level at which to obtain scalar relativistic corrections is further discussed in the Appendix.

Our standard basis sets for energy evaluation are termed 6-31+G(d) in the present work and contain some augmentations compared to the 6-31G(d) sets described above for geometry optimization: A primitive (3f) contracted to [1f][42] was added to the copper basis, while the chlorine basis was augmented by a diffuse s and p ($\alpha_{s,p} = 0.0483$) function. Furthermore, all energy evaluations were performed using spherical harmonics bases. Computed energies were converted to enthalpies at 298 K by adding contributions from *PV* work as for ideal gases and zero-point vibrational energies along with the temperature-dependent part of the vibrational energy according to equations for the harmonic oscillator. The frequencies used were those obtained with the B3LYP method.

For the reference RCCSD(T) energy calculations on the $CuCl_2$ molecule (based on geometries obtained with UCCSD(T)/TZD2P), large atomic natural orbital bases (termed ANO-L) were used. Copper was described by a primitive (21s,15p,10d,6f,4g) set[54] generally contracted to [6s,5p,4d,3f,2g], while for chlorine, a primitive (17s,12p,5d,4f) set[55] was generally contracted to [5s,4p,3d,1f].

Results and Discussion

In the current section focus is set on describing the structure and properties of the title compounds, and discussion of the quantum chemical methods has been kept to a minimum. For information about the methods and basis sets applied, readers are referred to the Computational Details section. A discussion of the accuracy of bending potentials as calculated with various quantum chemical methods can be found in the Appendix.

$CuCl_2$. A recent study based on data from laser-induced fluorescence (LIF) and laser excitation spectroscopy concluded that the ground state of $CuCl_2$ is $^2\Pi_g$ ($\delta^4\pi^3\sigma^2$) (Beattie et al.[24]). A theoretical investigation of linear $CuCl_2$ employing various size-consistent configuration interaction (CI) schemes and large basis sets has been reported by Bauschlicher and Roos[24] (BR). They found the ground state to be an almost equal mixture of $^2\Sigma_g^+$ ($\delta^4\pi^4\sigma^1$) and $^2\Pi_g$ when estimates of spin−orbit effects are included, the latter state being more stable by about 1.9 kcal/mol when spin−orbit effects are ignored. Indeed, the narrow spacing between $^2\Sigma_g^+$ and $^2\Pi_g$ is also reflected in the current work (cf. Table 1). Including correlation effects is seen to be important for the description of the $^2\Pi_g$ state, and thus for predicting the right order among the two lower states. Including a perturbative estimate of connected triples through the RCCSD(T) method brings the predicted relative stability of $^2\Sigma_g^+$ and $^2\Pi_g$ in excellent agreement with the CI results obtained by BR. Extrapolation of the correlation energy according to the PCI-*X* scheme[50] yields an excitation energy only slightly higher than the one given by BR when applied to the CCSD(T) energies ($X = 80$), thus indicating the robustness of the latter method which is chosen as the standard for calculating energies in the current work, as further discussed in the Appendix. While HF underestimates the stability of $^2\Pi_g$ by ~7 kcal/mol, B3LYP, perhaps somewhat surprisingly, apparently overestimates this stability by about the same amount. Even higher (15−20 kcal/mol) $^2\Sigma_g^+ \leftarrow {}^2\Pi_g$ excitation energies have been obtained with pure DFT methods.[56,57] The workhorse ab initio methods of the current study have not been chosen with the aim of obtaining very accurate optical transition energies, and strictly we cannot yet decide upon which of these results are to be trusted. However, the paper by BR is strengthened by the fact that their excitation energies for atomic copper as well as the electron affinities for Cl are in good agreement with experiment.

Table 1. Energies and Enthalpies (kcal/mol) Relative to the Educts $CuCl_2$ ($^2\Pi_g$) and $AlCl_3$[a]

		$CuAlCl_5$		Cu_2Cl_4	
	$CuCl_2$ ($^2\Sigma_g^+$) ΔE_e	ΔE_e	ΔH_{298}	ΔE_e	ΔH_{298}
ROHF	−5.0	−25.1	−24.3	−29.6	−29.0
MCPF	−0.5	−35.3	−34.5		
PCI-78	0.8	−38.2	−37.4		
RCCSD(T)	1.6	−35.1	−34.3	−39.4	−38.8
PCI-80	3.2	−37.7	−36.8	−41.8	−41.2
B3LYP	9.3	−26.0	−25.2	−27.2	−26.6
BP86[b]	15.9				
CPF[c]	1.9				
Raman[d]					−34.2
vis[d]					−36.8

[a] The calculated energies and enthalpies are obtained for geometries optimized using B3LYP within ideal symmetry. [b] Reference 56. [c] Reference 25. [d] Reference 3.

The bond distance (Table 2) of $CuCl_2$ seems to be fairly well reproduced by B3LYP with modest basis sets and, for both states, comes out 2−3 pm longer than the ones obtained by BR, and 5−6 pm longer than experiment.[24] HF does not include sufficient covalence, resulting in a bond distance more than 10 pm longer than the experimental value for the ground state.

So far, we have only considered a linear geometry for copper dichloride. Calculated potentials for bending of the lowest linear state ($^2\Pi_g$) can be found in Figure 1. The state shown ($^2B_2$) is the lower of the two ($^2B_2$ and $^2A_2$) derived from bending of $^2\Pi_g$, and stabilization through bending could be expected as

(49) Andersson, K.; Blomberg, M. R. A.; Fülscher, M. P.; Karlström, G.; Lindh, R.; Malmqvist, P.-Å.; Neogrády, P.; Olsen, J.; Roos, B. O.; Sadlej, A. J.; Schütz, M.; Seijo, L.; Serrano-Andrés, L.; Siegbahn, P. E. M.; Widmark, P.-O. MOLCAS, 4 ed.; Lund University: Lund, Sweden, 1997.
(50) Siegbahn, P. E. M.; Blomberg, M. R. A.; Svensson, M. *Chem. Phys. Lett.* **1994**, *223*, 35.
(51) Siegbahn, P. E. M.; Svensson, M.; Boussard, P. J. E. *J. Chem. Phys.* **1995**, *102*, 5377.
(52) Martin, R. L. *J. Chem. Phys.* **1983**, *87*, 750.
(53) Cowan, R. D.; Griffin, D. C. *J. Opt. Soc. Am.* **1976**, *66*, 1010.
(54) Pou-Amérigo, R.; Merchán, M.; Nebot-Gil, I.; Widmark, P.-O.; Roos, B. O. *Theor. Chim. Acta* **1995**, *92*, 149.
(55) Widmark, P.-O.; Persson, B. J.; Roos, B. O. *Theor. Chim. Acta* **1991**, *79*, 419.
(56) Deeth, R. J. *J. Chem. Soc., Dalton Trans.* **1993**, 1061.
(57) Rogemond, F.; Chermette, H.; Salahub, D. R. *Chem. Phys. Lett.* **1994**, *219*, 228.

Table 2. Calculated Geometry (Å, deg) and Vibrational Frequencies (cm^{-1})/IR Intensities (D^2 $Å^{-2}$ u^{-1}) for Linear $CuCl_2$ Compared to Experimental Vibrational Frequencies

method	ROHF	ROHF	UHF	B3LYP	B3LYP	obsd	
state	$^2\Sigma_g^+$	$^2\Pi_g$	$^2\Pi_g$	$^2\Pi_g$	$^2\Sigma_g^+$		
bond distance r(Cu−Cl)	2.144	2.140	2.139	2.090	2.110	2.035[a]	
mode				frequency/IR intensity			TED ($^2\Sigma_g^+$, ROHF)
ν_2 (Π_u)	112/1.41	81/0.70 108/0.63	80/0.70 108/0.62	71/0.21 118/0.16	71/1.07	127,[b] 130,[c] 96[a]	α, 100%
ν_1 (Σ_g^+)	358/0	350/0	349/0	332/0	343/0	360 ± 15,[d] 373,[b] 370,[c] 372[a]	*r*, 100%
ν_3 (Σ_u^+)	502/2.59	499/2.76	499/2.82	479/0.96	488/2.50	496 ± 20,[e] 503,[c] 526[a]	*r*, 100%

[a] Reference 24 (laser-induced fluorescence/molecular beam). [b] Reference 3 (Raman). [c] Reference 2 (resonance Raman). [d] Reference 58 (from vibronic structure in UV/vis spectrum). [e] Reference 1 (gas-phase IR).

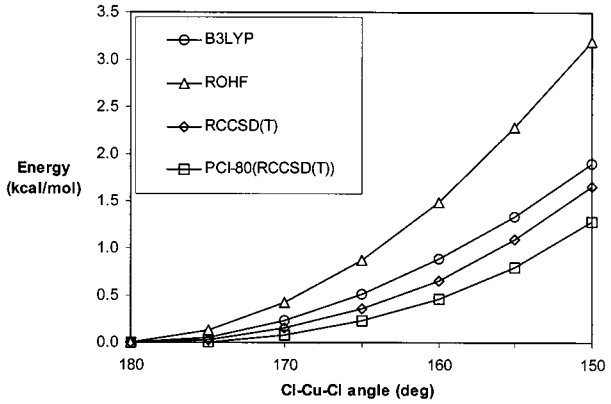

Figure 1. Calculated bending potentials for $CuCl_2$ with angles 180−150°. Estimates of scalar relativistic effects, as obtained from the MCPF density, included.

the only singly occupied d orbital is localized in the bending plane. For $^2A_2$, however, the singly occupied orbital is perpendicular to the bending plane, and no corresponding stabilization should be expected. On the other hand, bending of the $^2\Sigma_g^+$ state is not expected to induce stabilization, as doubly occupied orbitals are located in both possible bending planes, whereas the singly occupied orbital (σ_g^+) should favor a linear configuration. The last of the valence states, $^2\Delta_g$, may only experience reduced repulsion from the hole in the d shell at angles so sharp that repulsion between the ligands will dominate.

The $^2B_2$ curves in Figure 1 show that the molecule can be rather easily bent, at least at wide angles, and excluding HF (upper curve), there seems to be a nice agreement among the methods in predicting the shape of the curve. Both B3LYP and the two coupled cluster based methods shown predict that bending to reach 150° should cost less than 2 kcal/mol. The scheme where the correlation energy is extrapolated to include 100% of the correlation effects, PCI-80(RCCSD(T)), is expected to be the most accurate of the methods included in Figure 1, and has been shown to provide a bending potential in excellent agreement with coupled cluster calculations with large basis sets (cf. discussion in the Appendix). Furthermore, comparing the HF-based potential with the three correlated ones, it is clear that inclusion of correlation effects stabilizes bent structures, but the present curves of bending never actually fall below the level of a linear molecule. However, the energetical preference for a linear geometry is very small, and it is obvious that a more thorough correlation treatment as well as inclusion of spin−orbit and vibronic coupling may alter the detailed shape of the curve. What does seem clear, however, is that the potential curve for bending of the ground state of $CuCl_2$ is flat, and that the bending mode has a low frequency and a large amplitude.

The calculated frequencies (Table 2) are comparable with the observed values for the stretching modes. The scaling factors (averaged ratio between observed[2] and calculated frequencies) for the stretching modes are 1.01 and 1.05 for HF and B3LYP at the ground state, confirming that the calculated bonds are too weak (long) but that the deviation from experiment is not dramatic. The calculated ν_3 frequency differs significantly from the one reported by Beattie et al.[24] based on LIF measurements. At present we have no explanation for this deviation.

The Renner effects[59] expected for $^2\Pi_g$ and the apparent anharmonicity of the bending mode in this state (cf. Figure 1) make it difficult to compare observed fundamentals for this mode with the present harmonic frequencies obtained within the Born−Oppenheimer approximation. The observed band[2,3] at ∼130 cm^{-1} does not seem to correspond to the bending mode in $^2\Sigma_g^+$, as judged from the deviation from the present values for ν_2. Neither does it correspond very well with the calculated upper component of the bending mode in $^2\Pi_g$, and thus the recent value (96 cm^{-1}) reported by Beattie et al.[24] seems to be supported by the current calculations. The lack of an observed second component of the bending mode, however, suggests that the molecule is bent rather than linear.

Also interesting in this respect is the discrepancy between the spectroscopic results for $CuCl_2$: The Raman[3] and resonance Raman[2] spectra recorded some 20 years ago display intensive bands at ∼130 cm^{-1} that were attributed to the bending mode, as well as bands at ∼500 cm^{-1} assigned to either asymmetric stretch[2] or a combination $\nu_1 + \nu_2$.[3] The apparent Raman activity of ν_2 and ν_3 suggests a bent molecule, which also is the conclusion reached by both Dienstbach et al.[3] and Papatheodorou.[2] In contrast, Beattie et al.[24] recently claimed that $CuCl_2$ is linear, on the basis of analysis of data obtained with laser-induced fluorescence and laser excitation spectroscopy, although the isotopic shift pattern in fact indicated a slightly bent (173°) structure. Their conclusion is supported by the lack of an IR band corresponding to symmetric stretch. However, with the experimental difficulties—and with the perceived low IR intensity of ν_1 in a slightly bent molecule—this is not a very strong argument. Hence, although $CuCl_2$ has been studied intensively by various spectroscopic techniques, the results relevant for the shape of this molecule still appear to be rather confusing.

$CuAlCl_5$ and $CuGaCl_5$. The calculated geometries and vibrational frequencies for the two compounds are given in Tables 3 and 4, while energies relative to the educts $CuCl_2$ ($^2\Pi_g$) and $AlCl_3$ can be found in Table 1. The complexes display three-coordinate copper with two chlorines bridged to the tetrahedrally coordinated aluminum or gallium (Figure 2). The copper atom can be thought of as having an electron configuration similar to that of copper in the $^2\Pi_g$ ground state of $CuCl_2$ (described

(58) DeKock, C. W.; Gruen, D. M. *J. Chem. Phys.* **1966**, *44*, 4387.
(59) Renner, R. *Z. Phys.* **1934**, *92*, 172.

Table 3. Calculated Geometry (Å, deg) and Vibrational Frequencies (cm^{-1})/IR Intensities (D^2 $Å^{-2}$ u^{-1}) for $CuAlCl_5$ Compared to Experimental Vibrational Frequencies

method	ROHF	UHF	B3LYP		
symmetry	C_s	C_s	C_{2v}		
state	$^2A'$	$^2A'$	$^2B_2$		
geometry					
r_1' (Cu−Cl_b)	2.387	2.387	2.289		
r_1 (Cu−Cl_b)	2.319	2.316			
r_2' (Al−Cl_b)	2.248	2.246	2.273		
r_2 (Al−Cl_b)	2.297	2.297			
r_3 (Al−Cl_t)	2.092	2.092	2.102		
r_4 (Cu−Cl_t)	2.146	2.144	2.101		
B (Cu−Al)	3.271	3.270	3.188		
α (Cl_t−Al−Cl_t)	120.6	120.7	120.0		
β (Cu−Cl_b−Al)	89.8/90.3	89.7/90.3	88.6		
γ'/γ (Cl_b−Cu−Cl_t)	122.2/149.8	121.5/150.5	134.5		
θ (Cl_b−Al−Cl_t)	109.0/111.2	109.0/111.2	110.4		
ϵ (Al−Cu−Cl_t)	165.6	164.9	180		
mode		frequency/IR intensity		obsd	TED[a] (UHF)
ν_{15} (A″)	24/0.04	24/0.04	21/0.01 B_1		ζ, 85%; θ, 9%; μ, 6%
ν_{10} (A′)	59/0.29	62/0.28	18/0.07 B_2		γ, 100%
ν_{14} (A″)	96/0.22	96/0.21	95/0 A_2		μ, 71%; θ, 27%
ν_{13} (A″)	108/0.03	108/0.03	100/0.05 B_1		θ, 84%; γ, 15%
ν_9 (A′)	110/0.16	110/0.17	102/0.05 A_1		θ, 68%; B, 28%
ν_8 (A′)	152/0.08	153/0.08	148/0.10 B_2		θ, 78%; r_1/r_1', 22%
ν_{12} (A″)	177/0.35	177/0.35	161/0.18 B_1		θ, 77%; ζ, 13%; μ, 7%
ν_7 (A′)	191/0.04	191/0.04	178/0.15 A_1		B, 64%; θ, 31%
ν_6 (A′)	233/0.18	233/0.18	242/0.04 B_2		r_1/r_1', 68%; r_2/r_2', 23%; θ, 7%
ν_5 (A′)	289/0.97	289/0.97	272/1.02 A_1	291,[b] 289[c]	r_1/r_1', 85%; r_4, 6%
ν_4 (A′)	341/0.92	341/0.93	326/0.26 A_1		r_2/r_2', 78%; r_3, 16%; r_1/r_1', 7%
ν_3 (A′)	390/3.18	390/3.11	367/1.99 B_2		r_2/r_2', 69%; θ, 10%; r_1, 8%; r_3, 7%
ν_2 (A′)	443/3.46	444/3.49	419/1.69 A_1	448,[b] 444[c]	r_4, 84%; r_1, 11%
ν_1 (A′)	522/4.42	522/4.43	500/5.01 A_1		r_3, 69%; r_2/r_2', 22%; B, 5%
ν_{11} (A″)	628/5.04	628/5.04	599/4.04 B_1		r_3, 97%

[a] Contributions below 5% were omitted. [b] Reference 2. [c] Reference 15.

above), the hole in the d shell being assigned to the d_{xy} orbital in-plane with the bridging chlorines (cf. Figure 2).

A shallow potential for bending of chlorine in the plane of the singly occupied d orbital was observed in the calculations on $CuCl_2$, and it is interesting to check for a similar property also for the complexes containing three-coordinate copper. In fact, bending of the terminal chlorine in $CuAlCl_5$ is favored at the nonrelativistic HF level, resulting in a $^2A'$ ground state, while B3LYP predicts the symmetrically oriented terminal Cu−Cl bond, resulting in a $^2B_2$ ground state.

As for $CuCl_2$, B3LYP predicts somewhat shorter bonds than does HF, the difference being more pronounced for the bridges. The HF-optimized structures are seen to have unsymmetrical bridges due to a trans influence from the bent terminal Cu−Cl bonds. The energies and enthalpies of forming the $CuAlCl_5$ complex from the $CuCl_2$ and $AlCl_3$ educts (Table 1) show the expected stabilization of the product upon inclusion of correlation effects in the ab initio approach, while B3LYP somewhat surprisingly groups together with HF. There is considerable experience with MCPF as a useful tool for predicting energetics of reactions involving transition metals.[60] The stable performance normally obtained suggests that the ab initio correlated results probably are closer to reality than HF and B3LYP in this case. However, the absolute value for the reaction energy (enthalpy) is probably slightly exaggerated, as a Hartree−Fock limit correction is not included.

A closer look at the potentials for bending of the terminal Cu−Cl bond in the *xy* plane of $CuAlCl_5$ (Figure 3) reveals a remarkable similarity with the corresponding curves for $CuCl_2$ (Figure 1). These energy calculations were performed with a larger basis than the geometry optimizations, and also include scalar relativistic corrections as described in the Computational Details section and further discussed in the Appendix. The relativistic corrections disfavor bending, and at 150° this contribution amounts to 0.4 kcal/mol. With the relativistic effect included, HF, as well as the other methods included in Figure 3, predicts a C_{2v} symmetric geometry. The difference in energy compared to a 160° bent geometry is only some few tenths of a kilocalorie/mole, and bending to reach 150° costs less than 2 kcal/mol as also found for $CuCl_2$. Thus, one of the chlorines in $CuCl_2$ is seemingly only little affected by the increased coordination number of Cu through complexation with $AlCl_3$ ($GaCl_3$). Again, the conclusion must be that the bending mode for this terminal Cu−Cl bond is very soft, and it is at present not possible or meaningful to decide upon exactly where the minimum on the potential curve of bending is located.

The calculated frequencies compared with the experimental frequencies do not give any conclusive evidence as to whether the C_{2v} or C_s symmetry is correct for $CuAlCl_5$. The scaling factors are similar to those found for $CuCl_2$ and are internally consistent for both methods. The assignment of the bands given by Papatheodorou[2] is verified.

The ratio between the calculated frequencies obtained using HF and B3LYP is constant within ±1% for the modes with the six highest frequencies. Only for the seventh band is there a significant deviation, which probably is due to the different symmetries obtained with the two methods. Hence, the observation of this band may afford a distinction of the correct symmetry, although it might not be easily observed as the corresponding mode has low activity in IR, and probably also in Raman. All modes are both IR and Raman active for both

(60) Svensson, M. Ph.D. Thesis, Department of Physics, University of Stockholm, Stockholm, Sweden, 1994.

Table 4. Calculated Geometry (Å, deg) and Vibrational Frequencies (cm^{-1})/IR Intensities (D^2 $Å^{-2}$ u^{-1}) for $CuGaCl_5$ Compared to Experimental Vibrational Frequencies

method state	ROHF	UHF		
state	$^2A'$	$^2A''$		
geometry				
r_1' (Cu−Cl_b)	2.375	2.376		
r_1 (Cu−Cl_b)	2.312	2.309		
r_2' (Ga−Cl_b)	2.294	2.292		
r_2 (Ga−Cl_b)	2.351	2.353		
r_3 (Ga−Cl_t)	2.122	2.122		
r_4 (Cu−Cl_t)	2.148	2.146		
B (Cu−Ga)	3.288	3.287		
α (Cl_t−Ga−Cl_t)	122.4	122.4		
β (Cu−Cl_b−Ga)	89.5/89.7	89.5/89.7		
γ'/γ (Cl_b−Cu−Cl_t)	122.9/147.2	121.9/148.2		
θ (Cl_b−Ga−Cl_t)	108.6/110.8	108.5/110.9		
ϵ (Ga−Cu−Cl_t)	167.2	166.1		
mode	frequency/IR intensity		obsd	TED[a] (ROHF)
ν_{15} (A'')	21/0.03	21/0.03		ζ, 86%; θ, 12%
ν_{10} (A')	54/0.23	58/0.22		γ, 100%
ν_{14} (A'')	93/0.14	93/0.14		μ, 65%; θ, 35%
ν_9 (A')	102/0.14	102/0.14		θ, 67%; B, 31%
ν_{13} (A'')	103/0.03	103/0.03		θ, 83%; μ, 17%
ν_8 (A')	123/0.20	124/0.20		θ, 87%; r_1/r_1', 10%
ν_{12} (A'')	154/0.47	154/0.47		θ, 69%; μ, 16%; ζ, 15%
ν_7 (A')	159/0.20	159/0.20		B, 64%; θ, 34%
ν_6 (A')	226/0.01	226/0.02		r_1/r_1', 49%; r_2/r_2', 45%
ν_5 (A')	268/2.25	267/2.29	278[b]	r_1/r_1', 58%; r_2/r_2', 38%
ν_4 (A')	306/1.22	306/1.14		r_1/r_1', 60%; r_2/r_2', 30%; r_4, 7%
ν_3 (A')	324/1.08	325/1.08		r_2/r_2', 88%; r_1/r_1', 12%
ν_2 (A')	420/2.81	420/2.79		r_3, 90%; r_4, 8%
ν_1 (A')	444/1.28	444/1.33	443[b]	r_4, 80%; r_1/r_1', 10%; r_3, 8%
ν_{11} (A'')	487/2.48	487/2.48		r_3, 100%

[a] Contributions below 5% were omitted. [b] Reference 15.

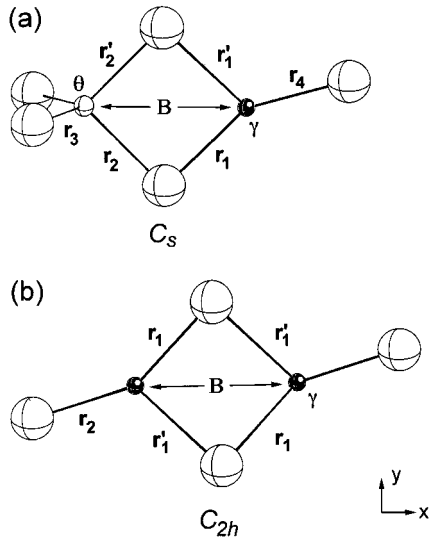

Figure 2. Structures of the $CuAlCl_5$ complex (a) and Cu_2Cl_4 dimer (b). Also shown are the internal coordinates, except for the terminal out-of-plane bend μ (Cl_t−Cu−2Cl_b) and the ring torsion ζ (Cu−Cl_b−Cl_b−Al/Cu).

symmetries, except for the IR-inactive A_2 mode in C_{2v} symmetry, where the equivalent C_s mode ν_{14} (A'') has a low intensity as well. Therefore, one should not expect conclusive changes in intensities or Raman polarizabilities due to a minor deviation from a C_{2v} symmetry.

For $CuGaCl_5$ only geometry optimizations and frequency calculations at the HF level are reported. As the optimized angle Ga−Cu−Cl_t is only a couple of degrees wider and the in-plane bending mode of the terminal Cl (ν_{10}) has an even lower frequency than in the aluminum complex, it is reasonable to

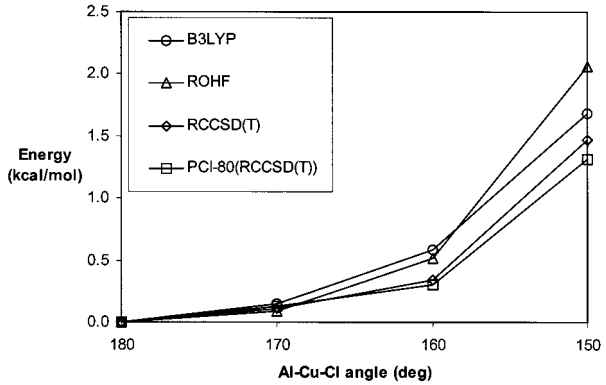

Figure 3. Calculated bending potentials for $CuAlCl_5$ with angles 180−150°. Estimates of scalar relativistic effects, as obtained from the MCPF density, included.

assume that the conclusions reached above based on the bending potentials of $CuAlCl_5$ should be valid also for the gallium complex.

The calculated frequencies fit reasonably well to the observed frequencies for $CuGaCl_5$,[15] but the deviation for the symmetric Cu−Cl_b stretch is larger than expected. Also, the difference between the $CuGaCl_5$ and the $CuAlCl_5$ frequencies for ν_5 is much overestimated by the calculations. This could signal an inaccuracy in the calculated value or even an erroneous interpretation of the vibrational spectrum given by Schläpfer and Rohrbasser.[15]

Cu_2Cl_4. The calculated geometries and vibrational frequencies are given in Table 5, while energies relative to the educts can be found in Table 1. The calculations show a three-coordinate copper, with an environment similar to that found in $CuAlCl_5$ and $CuGaCl_5$ (Figure 2).

Table 5. Calculated Geometry (Å, deg) and Vibrational Frequencies (cm^{-1})/IR intensities (D^2 $Å^{-2}$ u^{-1}) for Cu_2Cl_4 Compared to Experimental Vibrational Frequencies

method	ROHF	UHF	B3LYP		
state	^3B_u	^3B_u	^3B_u		
geometry					
r_1 (Cu−Cl_b)	2.294	2.291	2.269		
r_1' (Cu−Cl_b)	2.390	2.390	2.285		
r_2 (Cu−Cl_t)	2.154	2.152	2.109		
B (Cu−Cu)	3.290	3.288	3.184		
β (Cu−Cl_b−Cu)	89.2	89.2	88.7		
γ'/γ (Cl_b−Cu−Cl_t)	120.1/149.1	119.3/149.9	125.6/143.1		
ϵ (Cu−Cu−Cl_t)	165.5	164.7	171.1		
mode		frequency/IR intensity		obsd	TED[a] (UHF)
ν_7 (A_u)	30/0.11	30/0.10	29/0.01		ζ, 73%; μ, 27%
ν_{12} (B_u)	61/0.42	63/0.41	25/0.08		γ, 96%
ν_5 (A_g)	70/0	73/0	46/0		γ, 99%; r_1', 7%; r_1, 3%
ν_8 (B_g)	95/0	96/0	99/0		μ, 100%
ν_4 (A_g)	130/0	130/0	123/0	165[b]	B, 100%
ν_6 (A_u)	136/0.94	137/0.93	127/0.28		μ, 73%; ζ, 27%
ν_3 (A_g)	220/0	220/0	249/0		r_1', 75%; r_1, 21%
ν_{11} (B_u)	249/1.98	248/2.02	270/0.55		r_1', 94%
ν_{10} (B_u)	304/1.04	305/0.97	284/0.61		r_1, 82%; r_2, 14%
ν_2 (A_g)	307/0	308/0	294/0	314[c], 307[b]	r_1, 71%; r_1', 22%; r_2, 10%
ν_9 (B_u)	435/5.07	436/5.12	414/2.87		r_2, 85%; r_1, 15%
ν_1 (A_g)	444/0	445/0	423/0	442,[c] 443[b]	r_2, 85%; r_1, 11%

[a] Contributions below 5% were omitted. [b] Reference 3. [c] Reference 2.

Without effects from relativity both HF and B3LYP predict a ^3B_u ground state with equilibrium structures that can be described as being distorted to C_{2h} from the (ideal) D_{2h} symmetry due to bending of the terminal chlorines in the plane of the singly occupied orbitals.

As for $CuCl_2$ and the two complexes with main group metal trichlorides, B3LYP predicts somewhat shorter bonds than does HF, and this difference is more pronounced for the bridges. The bridges are furthermore seen to be unsymmetrical due to a trans influence from the bent terminal Cu−Cl bonds, but with a difference in the bridging bond lengths of less than 2 pm in the B3LYP-optimized structure. The energies and enthalpies of dimerization (Table 1) show that, as for $CuAlCl_5$, B3LYP groups together with HF, and predict too low absolute values. As expected when basis set corrections are not included in correlated ab initio calculations of bond strengths, the predictions from coupled cluster are located rather on the higher side of experiment. Inclusion of such corrections would probably bring the latter estimates in good agreement with at least the experimental value from visible spectroscopy.[3] For technical reasons, we were not able to carry out MCPF calculations on Cu_2Cl_4.

The HF and B3LYP potential curves of bending (Figure 4) both indicate a weak stabilization through distortion to C_{2h} symmetry, whereas the two curves based on the coupled cluster approximation predict the more symmetric D_{2h} structure with a $^3B_{1u}$ ground state to be preferred. Thus, on going from the monomer to the bridged complexes, one may notice an increased preference for bending of the terminal chlorines at the HF and B3LYP levels. Our more accurate estimates (based on coupled cluster), however, predict that the shape of the bending potential essentially stays constant. It seems reasonable to attribute this difference to an increased exaggeration of the ionic contributions to the bonds on going from the monomer to the bridged complexes at the SCF (HF and B3LYP) levels. At the ionic limit, d electrons are antibonding, and complexes will tend to adopt conformations minimizing Pauli repulsion. In all of the current complexes there are significant covalent contributions, and forming the best possible directional (and d-rich) bonds seems to be more important than a mere avoidance of repulsion.

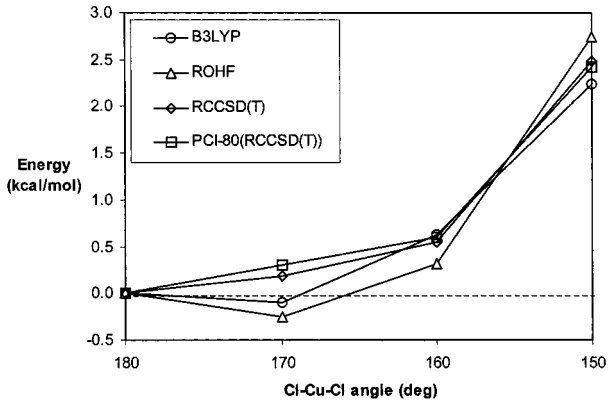

Figure 4. Calculated bending potentials for Cu_2Cl_4 with angles 180−150°. Estimates of scalar relativistic effects, as obtained from the ROHF density, included.

The calculated vibrational frequencies correspond well with the observed frequencies, if the same scaling factors as for the monomer are adopted: 1.01 for the HF calculations and 1.05 for the B3LYP calculations. In fact, the similarity between the scaling factors for the individual modes is convincing. The total energy distribution (TED) values also verify the assignments given by Papatheodorou.[2]

An early report[1] gave a frequency for ν_9 (416.5 ± 5 cm^{-1}) differing from the calculated value by ca. 20 cm^{-1} (after scaling). However, it is very difficult to evaluate the reliability of the experimental value on basis of the data given in the report, and we have found no other reports on this IR band. Also, the correspondence between the HF and B3LYP frequencies for this mode indicates that a new investigation of the IR spectrum could be useful.

It should be noted that a forced D_{2h} symmetry yields a slightly lower calculated frequency for this mode, but this shift accounts for only ∼20% of the discrepancy. A Raman band at 165 cm^{-1} reported by Dienstbach et al.[3] does not correspond to any calculated frequency from this work and is not verified by Papatheodorou.[2]

The few bands observed in Raman do not discriminate between ideal and distorted structures of Cu_2Cl_4. An observation

of ν_6 (A_u) in IR should be diagnostic as it is not active in D_{2h} symmetry. Also the difference between the two B_{2u} modes ν_{10} and ν_{11} seems to be very sensitive to the distortion (cf. the HF and B3LYP values) and could give valuable, or even conclusive, information.

Conclusion

We have seen that all Cu d^9 complexes in the current study are predicted by our most accurate ab initio methods to adopt their expected, ideal symmetries. The terminal chlorines attached to copper may, however, easily be bent, causing the energetical preference for ideal structures to be rather tiny. Hence, it is still possible that effects not accounted for in the present study might change the picture in favor of the more unsymmetric structures. The most important finding regarding the orientation of the terminal chlorines is thus simply that the force constant for bending of the latter is close to zero. The ease with which these complexes can be distorted may be understood by considering the reduced repulsion from the singly occupied π_g orbital in the lower linear state, $^2\Pi_g$ ($\delta^4\pi^3\sigma^2$), of the monomer. A similar electron configuration, facilitating bending of terminal chlorines in a plane of symmetry, is also found for the ground states of the higher associates of $CuCl_2$.

The present work has also shown that calculation of accurate bending potentials for two- and three-coordinate transition metal complexes is a difficult task. On several occasions HF, B3LYP, and MCPF predicted structures of lower symmetry than obtained with CCSD(T).

The vibrational analyses confirm most existing interpretations of the vibrational spectra, but on some occasions reinterpretations are suggested. The calculations also give hints to bands that may facilitate the verification of the structures, and it appears that IR spectra may be more diagnostic than Raman spectra.

Acknowledgment. The project benefited from grants of computing time from The Research Council of Norway (NFR, Programme for Supercomputing). Some of the calculations were performed on the Intel Paragon at SINTEF, Trondheim, which was supported in part by Intel Corporation through the SINTEF/Intel Paragon Supercomputer Partnership Agreement. B.K.Y. acknowledges a scholarship from the NTNU, while V.R.J. acknowledges VISTA (Grant V6415), NFR (Grant 119204/410), and Max-Planck-Institut für Kohlenforschung for financial support.

Appendix. Evaluation of the Level of Calculation

The effects of including higher excitations and improving the basis sets were studied for the monomer, $CuCl_2$. For this task, we needed to establish a "best estimate" for the bending potential of the ground state, which among other things involved obtaining geometries of better quality than our standard B3LYP/6-31G(d) set.

The Cu−Cl bond length of the $^2\Pi_g$-derived $^2B_2$ ground state was optimized at the UCCSD(T)/TZD2P level for Cl−Cu−Cl angles in the range 180−150°. As expected, this resulted in somewhat shorter bonds than optimized with B3LYP/6-31G(d), and for the linear case a distance (2.072 Å) in better agreement with the presumably most accurate optimization by BR (2.056 Å). The more accurately obtained geometries were subsequently used in coupled cluster energy calculations with a large ANO basis (ANO-L), to give what in the present work is regarded as the highest quality bending potential, the RCCSD(T)/ANO-L curve in Figure A1. The agreement between the ANO-L based

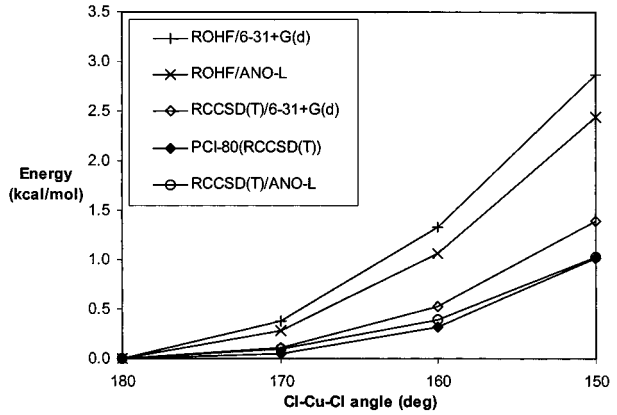

Figure A1. Calculated bending potentials for $CuCl_2$ with angles 180−150°, using 6-31+G(d) and ANO-L bases as indicated. The 6-31+G(d) energies are calculated for B3LYP/6-31G(d)-optimized Cu−Cl bond lengths, while for ANO-L the bond lengths were taken from UCCSD(T)/TZD2P optimizations. Relativistic effects are not included.

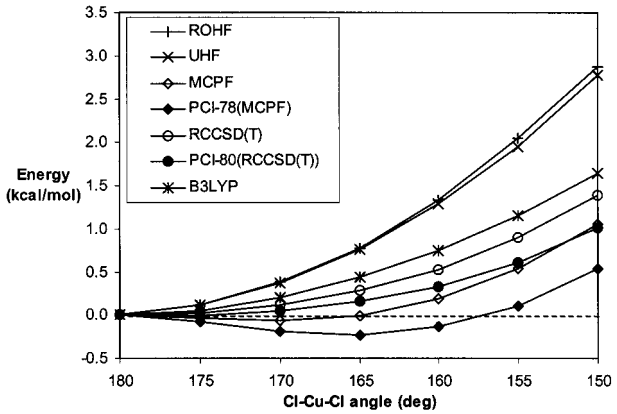

Figure A2. Calculated bending potentials for $CuCl_2$ with angles 180−150°, using 6-31+G(d) bases. Relativistic effects are not included.

energies and the extrapolated RCCSD(T)/6-31+G(d) results suggests that the latter, far less involving, calculations can be trusted also for the larger complexes in the present study, and as such represents an important result. The fact that the two curves almost overlap, however, is somewhat coincidental. The main reason is that the present PCI-80 energies do not include HF-limit corrections, as calculation of the latter was not deemed practical for the higher complexes. The moderate difference between the 6-31+G(d) and ANO-L HF curves shows that these corrections are small, but including them would still lead to a slight departure from the RCCSD(T)/ANO-L line.

Having established that the PCI-80 curve from extrapolation of RCCSD(T)/6-31+G(d) energies seems to be a reasonable approximation to the bending potentials involving much larger bases, we set out to compare the PCI-80 results with calculations employing a range of contemporary methods. Using our standard B3LYP/6-31G(d)-optimized geometries, single point energy calculations were performed with MCPF, coupled cluster based on both restricted and unrestricted reference, and B3LYP. 6-31+G(d) bases were used for these calculations, and the most important of the thus obtained bending potentials are shown in Figure A2.

Only a minor effect of going from a restricted to an unrestricted formulation is evident when comparing the ROHF and UHF results in Figure A2. The effect of changing from a restricted to an unrestricted reference in the coupled cluster calculations is even smaller. Also, the effect of including

perturbative corrections from connected triples was found to be very small, and thus among the coupled cluster results only the RCCSD(T) and corresponding extrapolated PCI-80 curves are shown. Comparing the HF curves with the ones derived from correlated methods, it is clear that inclusion of correlation effects in general contributes to stabilization of bent structures. However, only the two MCPF-based curves are actually predicting that bent structures should be more stable than the linear molecule, and they are located significantly below our best estimate, PCI-80(CCSD(T)).

MCPF is not formally invariant to rotations that mix occupied (or virtual) orbitals among themselves. The unexpected deviation from the coupled cluster curves may be a sign that the orbital variance problem influences the present MCPF-derived bending potentials, and hence no bending potentials obtained at this level are included in the Results and Discussion section of the present contribution.

It seems as if the hybrid method included, B3LYP, is able to describe the bending of $CuCl_2$ fairly well and at least represents a significant improvement over the HF methods in this respect. The method, however, predicts too much destabilization of the bent structures compared to PCI-80, and should be accompanied by other methods when studying bending of the larger complexes.

In this section, we have so far only compared nonrelativistic energies. For a more complete picture of the variation of the total energy upon bending, some estimate of the influence of relativity should be included. Figure A3 shows how scalar relativistic corrections, as obtained at the ROHF and MCPF levels and with different basis sets, vary along with bending of the $CuCl_2$ molecule. It is immediately clear that relativity in general contributes to destabilization of bent structures, but that these effects are rather small. At 150° (170°), the estimates of destabilization through relativity compared to the linear case are all lower than 0.5 (0.1) kcal/mol. The MPCF/TZD2P alternative, which predicts the largest destabilization of the bent structures, is too costly for the higher complexes in this study. The disagreement between MCPF/TZD2P and the corresponding ROHF results also appears to be somewhat unusual, see, e.g., Espelid et al.[61] The corrections based on ROHF/6-31+G(d) stand out as too low, while there seems to be a nice agreement among the three curves in the middle, namely, the corrections based on ROHF/TZD2P, ROHF/ANO-L, and MCPF/6-31+G(d), and for simplicity the latter approach was chosen as the standard in the present work. However, for technical reasons it turned out that no MCPF calculations for Cu_2Cl_4 could be performed,

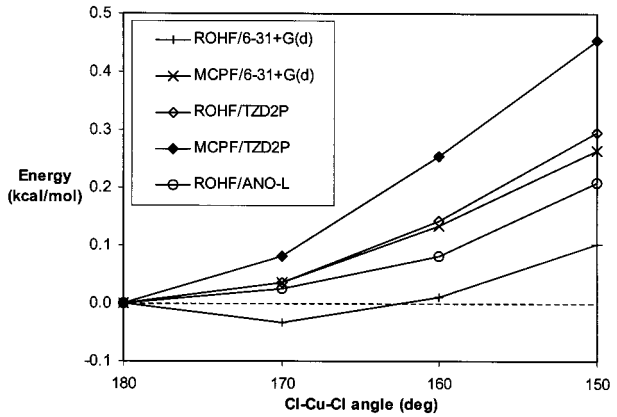

Figure A3. Scalar relativistic corrections calculated for $CuCl_2$ with angles 180−150°. The 6-31+G(d) energies are calculated for B3LYP/6-31G(d)-optimized Cu−Cl bond lengths, while for ANO-L the bond lengths were taken from UCCSD(T)/TZD2P optimizations.

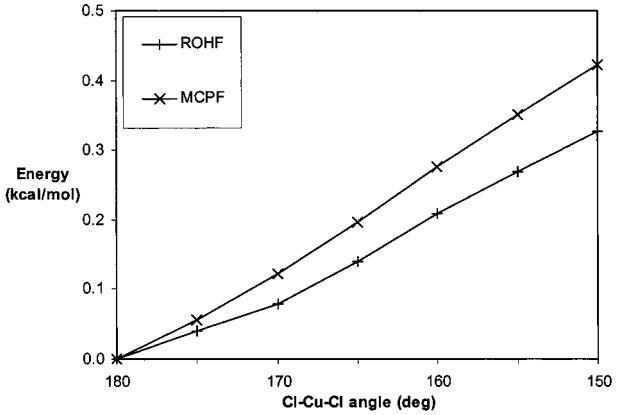

Figure A4. Scalar relativistic corrections calculated for $CuAlCl_5$ with angles 180−150°. The calculations were performed with 6-31+G(d) bases using B3LYP/6-31G(d)-optimized Cu−Cl bond lengths.

and for this molecule the corresponding ROHF-derived corrections were used instead. According to the results for $CuCl_2$ as shown in Figure A3, this should lead to too small corrections for bent structures. Thus, it may be of interest to check the validity of this approach by comparing ROHF- and MCPF-derived corrections also for $CuACl_5$, as given in Figure A4. It is immediately clear that the correlated and uncorrelated estimates of the scalar relativistic effects are closer for this molecule than for the monomer, and it is reasonable to believe that this will be the case also for the other bridged complex, Cu_2Cl_4.

IC990270M

(61) Espelid, Ø; Børve, K. J.; Jensen, V. R. *J. Phys. Chem. A* **1998**, *102*, 10414.